Phononic supercrystal as a highly absorbing metamaterial

Martin Ibarias ** and José Sánchez-Dehesa ** **

Wave Phenomena Group, Department of Electronic Engineering, Universitat Politècnica de València, Camino de vera s/n (Building 7F), ES-46022 Valencia, Spain

Arkadii Krokhin 🏻 ‡

Department of Physics, University of North Texas, P. O. Box 311427, Denton, Texas 76203, USA



(Received 3 April 2024; accepted 19 September 2024; published 4 October 2024)

We demonstrate analytically, numerically, and experimentally that a 2D supercrystal (SC)—an elastic structure of solid rods with two distinct spatial periods embedded in a viscous fluid—exhibits very high acoustic absorption. Smaller diameter rods arranged in a 2D lattice with a smaller period serve as an effective medium with high viscosity for a set of larger rods arranged in a lattice of much larger period. The enhancement of acoustic absorption is due to strong viscous friction within a narrow layer with high gradients of velocity formed around each scatterer. The SC as a whole is considered in the homogenization limit of frequencies where it behaves as a metafluid with an effective speed of sound and effective viscosity. Analytical results for the effective parameters are calculated for any Bravais lattices and arbitrary cross-sections of the rods. Experimental measurements of acoustic absorption in a supercrystal with hexagonal lattices for both types of rods are in a good agreement with analytical and numerical results.

DOI: 10.1103/PhysRevResearch.6.L042005

Viscous dissipation in fluids is caused by frictionlike forces acting between the layers of fluid moving with different velocities. A homogeneous fluid weakly absorbs propagating sound wave since velocities of vibrating fluid elements smoothly change at the wavelength scale λ . Much larger velocity gradients appear within a narrow boundary layer $\delta << \lambda$ formed near fluid-solid interface where fluid sticks to solid surface [1]. Damping of acoustic or elastic wave may be enhanced within relatively narrow range of frequencies near mechanical resonance [2-4]. The absorption band may be broaden due to inclusion of thermoviscous losses and combination of different structural elements like graded phononic crystal [5–7], resonators with spatial symmetry [8] or coherent coupling [9], porous and perforated media [10-12], and onmidirectional trapping of acoustic wave into phononic black hole [13].

The constituents of most effective wave absorbers are not necessarily the materials with high energy losses. Multiple interactions with scatterers and their specific geometry may lead to essential increase of absorption. Enhanced electromagnetic absorption at certain values of filling fraction was theoretically predicted for a 2D photonic crystal with complex-valued constituents [14]. The acoustic counterpart of this effect was demonstrated for the imaginary part of the effective

Published by the American Physical Society under the terms of the Creative Commons Attribution 4.0 International license. Further distribution of this work must maintain attribution to the author(s) and the published article's title, journal citation, and DOI.

mass density in a homogenized multi-scale phononic crystal of solid cylinders in air [15] and in a multilayered elastic structure [16].

Absorbance of a phononic crystal is much higher than the absorbance of its viscous background due to formation of a boundary layer around each scatterer. In the low-frequency limit a phononic crystal behaves as a homogeneous medium with effective parameters. The homogenization theory of 2D phononic crystal with viscous background was developed in Ref. [17]. Calculations of the decay coefficient of sound for several 2D lattices show that the boundary-layer effect may increase viscous decay of sound by 2-3 orders of magnitude [17,18]. A homogenized lossy phononic crystal can be considered as a metafluid with enhanced and anisotropic viscosity. The latter property is realized in the crystals with lower than 3-fold rotational symmetry. A theory of lossy solid-fluid superlattice valid at any frequency was recently proposed in Ref. [19].

A supercrystal (SC) is an artificial two-scale periodic structure where some properties attributed to photonic or phononic crystals may be enhanced. One-dimensional supercrystal serves as a model for periodic porous medium [20]. A layered supercrystal where the unit cell contains a layer of a regular dielectric and a layer of hyperbolic metamaterial presented by a homogenized multi-layered metallic sequence is a 1D hypercrystal [21]. Due to presence of the hyperbolic constituent, a photonic hypercrystal supports propagation of an unusual surface mode, which turns out to be a mixture of Tamm state and surface plasmon. Three-dimensional supercrystals were fabricated by packing clusters of gold nanoparticles in 3D periodic lattice [22]. Colloidal crystals organized in a diamond-like lattice represent 3D phononic supercrystal possessing an extremely wide band gap [23].

^{*}Contact author: maibaal1@eln.upv.es [†]Contact author: jsdehesa@upv.es

[‡]Contact author: arkady@unt.edu

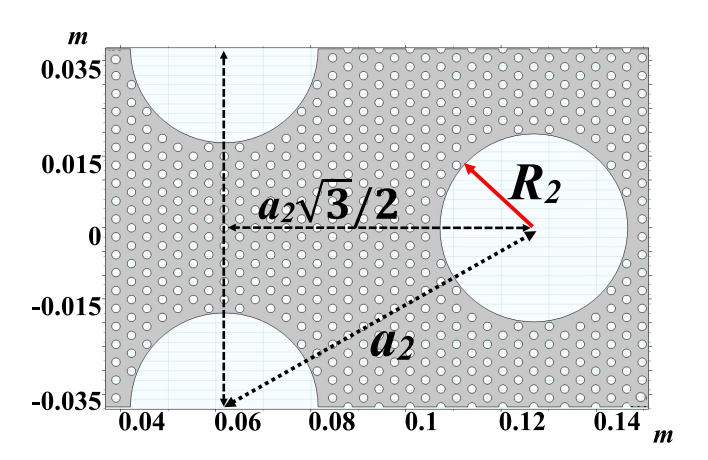


FIG. 1. 2D supercrystal of cylindrical rods in air. Small cylinders of radius $R_1=0.88169$ mm arranged in a hexagonal lattice with period $a_1=3.755$ mm. These small rods form a background for the hexagonal lattice of larger rods with $R_2=19.715$ mm and $a_2=20a_1=75.1$ mm. Both lattices have close filling fractions: $f_1=0.2$ and $f_2=0.25$.

Here we propose a phononic SC with air background which exhibits anomalously strong acoustic absorption within a wide band of frequencies. Figure 1 shows that at the larger scale, the SC looks as a set of large solid cylinders arranged in a hexagonal lattice with period a_2 . Unlike acoustic black-hole metamaterials, where enhanced absorption is due to the redirection of the incident waves towards the phononic crystal core with multiple narrow channels where viscous dissipation takes place [13], sound wave in supercrystal is absorbed due to multiple reflections from solid scatterers of essentially different size. The frequency of sound is supposed to be well below the first bandgap where effective parameters for speed of sound, mass density, and decay coefficient can be introduced. The background for these large solid scatterers is not directly air but a set of smaller cylinders also arranged in the hexagonal lattice with much shorter period a_1 . They form a viscous metafluid background for the larger cylinders. Due to two-scale periodicity there is a two-step enhancement of acoustic absorption. We report analytical, numerical, and experimental results for attenuation of sound in a hexagonal SC. The experimental results are obtained by measuring acoustic transmission and absorption of a supercrystal of acrylonitrile butadiene styrene (ABS) plastic cylinders in air. All the reported results are in a good agreement with each other.

In a homogeneous fluid acoustic pressure decays exponentially with distance, $p(x) \propto e^{-\gamma_0 x}$. Contribution of viscous dissipation to the attenuation coefficient is given by $\gamma_0 = \omega^2(\frac{4}{3}\eta_0 + \xi_0)/2\rho_0c_0^3$, where $\omega/2\pi$ is the wave frequency, ρ_0 , ρ_0 , ρ_0 , and ρ_0 are the fluid density, speed of sound, and viscosity coefficients. A sound wave propagating through a 2D lattice of solid rods losses its energy mainly within a narrow boundary layer of thickness $\delta = \sqrt{2\eta_0/(\rho_0\omega)}$ formed around each rod. The necessary condition for sound wave to propagate through a set of solid scatterers is $\delta << \lambda = 2\pi c_0/\omega$. The relative energy loss on the lattice period ρ_0 due to interaction with a single rod of circumference ρ_0 is ρ_0 . The attenuation coefficient is the relative energy loss per unit length. For 2D phononic crystal

it can be estimated as $\gamma_{ph} \sim \Delta E/aE \sim \frac{L}{a^2} \sqrt{\frac{\omega\eta_0}{\rho_0}} \sim \frac{1}{ac_0} \sqrt{\frac{f\omega\eta_0}{\rho_0}}$. Here $f \sim (L/a)^2$ is the filling fraction of solid scatterers in 2D lattice. This simple, order of magnitude estimate ignores contribution of inter rods scattering, specific shape of the rod's cross-section, and geometry of the unit cell. Using expansion over plane waves, the asymptotically exact result for γ_{ph} was obtained in the low-frequency limit, where dispersion relation is linear, $\omega = c_{\rm eff} k$ [17]. The effective speed of sound $c_{\rm eff}$ for solid-fluid phononic crystal was calculated in Refs. [24–26]. Due to natural anisotropy of crystal lattice the exact decay coefficient depends on the direction of propagation $\hat{\bf k} = {\bf k}/k$. The microstructure of the crystal enters to γ_{ph} through a numerical coefficient $M(\hat{\bf k}, \rho_0)/N(\hat{\bf k}, \rho_0)$ [27],

$$\gamma_{ph}(\hat{\mathbf{k}}) = \frac{L}{2A_c c_{\text{eff}}(\hat{\mathbf{k}})} \sqrt{\frac{\omega \eta_0}{2\rho_0}} \frac{M(\hat{\mathbf{k}}, \rho_0)}{N(\hat{\mathbf{k}}, \rho_0)}.$$
 (1)

Here the dimensionless quantities $M(\hat{\mathbf{k}}, \rho_0)$ and $N(\hat{\mathbf{k}}, \rho_0)$ are represented by some cumbersome series over reciprocal lattice vectors G [17]. These series contain the bulk form-factor

$$F(\mathbf{G}) = \frac{1}{A_c} \int_{a} e^{-i\mathbf{G} \cdot \mathbf{r}} d\mathbf{r}, \tag{2}$$

where A_c is the area of the unit cell and integration runs over the cross-section of the solid rod a. This form-factor defines the Fourier coefficients of any periodic function in a crystal lattice. Since dissipation occurs within the boundary layer, there is one more form-factor related to the periodic 2D structure of contours l_a separating solid rods from fluid environment

$$L(\mathbf{G}) = \frac{1}{L} \oint_{l_a} e^{-i\mathbf{G} \cdot \mathbf{r}} dl.$$
 (3)

At small filling fractions, the decay coefficient exhibits square-root singularity due to the factor $\sqrt{L^2/A_c} \sim \sqrt{f}$. At moderate and high fillings, the fraction $M(\hat{\mathbf{k}})/N(\hat{\mathbf{k}})$ grows fast with the filling fraction leading to strongly enhanced viscous losses [17,18].

In the frequency region where both lattices homogenize, Eq. (1) with the appropriate values of the effective density and speed of sound is applied for calculation of the decay coefficient of each set of cylinders and the SC as a whole. The homogenization condition $\lambda \ge 4a_2$ [25] is satisfied for frequencies up to 1 kHz lying well below the first band gap at 1.6 kHz. Of course, at these frequencies the lattice with period a_1 also behaves as a homogeneous medium. Thus the whole SC homogenizes.

Due to the threefold rotational symmetry the homogenized SC becomes acoustically isotropic in the low-frequency limit [24]. Dissipation of acoustic energy occurs mainly within the narrow boundary layer formed around each big and small cylinder. The neighboring boundary layers do not overlap if the filling fractions are not close to the corresponding close packing values. In this case, both lattices give additive contributions to the total decay coefficient of the SC

$$\gamma_{\rm sc} = \gamma_1 + \gamma_2,\tag{4}$$

similar to the contributions of distinguishable scatterers to resistance of metal (Matthiessen's rule). While two contributions to dissipation of sound are independent, each decay coefficient in Eq. (4) depends on the parameters of both lattices. Sound wave interacts with big and small cylinders that leads to additional enhancement of dissipation in supercrystal. Due to inter-lattice scattering each decay coefficient in Eq. (4) exceeds the decay coefficient in the corresponding phononic crystal containing one type of cylinders in air, i.e., $\gamma_1 > \gamma_{ph1}$ and $\gamma_2 > \gamma_{ph2}$. The decay coefficient γ_{ph1} (γ_{ph2}) is calculated directly from Eq. (1) by substituting the geometrical parameters of the lattice with period a_1 (a_2) and the physical parameters of air background: $\eta_0 = 1.85 \times 10^{-5}$ kg/(s m), $\rho_0 = 1.29 kg/m^3$, and $c_0 = 344 m/s$. Since the aluminum cylinders in air behave as hard scatterers, their elastic parameters can be omitted. The calculated decay coefficient in the lattice with period a_1 (a_2) is $\gamma_{ph1} = 0.004 \sqrt{\omega} \,\mathrm{m}^{-1}$ ($\gamma_{ph2} =$ $2.35 \times 10^{-4} \sqrt{\omega} \text{ m}^{-1}$) [27]. Scattering at solid cylinders leads to five orders of magnitude stronger decay than that in free air. For example, at frequency 250 Hz, $\gamma_{ph1}/\gamma_0 = 2.58 \times 10^5$.

The decay due to small cylinders is further enhanced in the SC. In the homogenized SC the small cylinders are imbedded not in air but in the elastic effective medium which replaces the phononic crystal of big cylinders in air. The effective parameters of the last medium, $c_{\text{eff2}} = 308 \text{ m/s}$ and $\rho_{\rm eff2} = 2.15 \text{ kg/m}^3$, are calculated using the theory proposed in Refs. [24,25,28]. The decay coefficient due to the small cylinders in the SC is calculated from Eq. (1) where $c_{\rm eff}$ is replaced by speed of sound in the SC $c_{\rm sc} = 281$ m/s and the mass density ρ_0 in the arguments of N and M is replaced by $\rho_{\rm eff2}$. The mass density under the square root in Eq. (1) remains ρ_0 since this factor originates from the thickness of the boundary layer, which is defined by the density of air. The calculated contribution of the small cylinders to the decay in the SC turns out to be 12.5% higher than the decay coefficient γ_{ph1} in the corresponding phononic crystal,

$$\gamma_1 = \frac{L_1}{2A_{c1}c_{sc}} \sqrt{\frac{\omega\eta_0}{2\rho_0}} \frac{M(\rho_{eff2})}{N(\rho_{eff2})} = 0.0045\sqrt{\omega} \text{ m}^{-1}.$$
 (5)

The contribution γ_2 of the big cylinders to the decay of sound in the SC is similarly calculated. The big cylinders are imbedded in a metafluid originated from the homogenized lattice of small cylinders. The effective mass density of this metafluid is $\rho_{\rm eff1} = 1.94 \ \rm kg/m^3$ and speed of sound $c_{\rm eff1} = 314 \ \rm m/s$. The speed of sound in the lattice of big cylinders with metafluid background of density $\rho_{\rm eff1}$ is the same as the speed of sound in the lattice of small cylinders with metafluid background of density $\rho_{\rm eff2}$, i.e., it is $c_{\rm sc}$. This symmetry is a property of the homogenized SC where any set of the cylinders may serve as a background for the other one. The decay coefficient γ_2 can now be written in the form similar to Eq. (5)

$$\gamma_2 = \frac{L_2}{2A_{c2}c_{sc}} \sqrt{\frac{\omega\eta_0}{2\rho_0}} \frac{M(\rho_{eff1})}{N(\rho_{eff1})} = 2.6 \times 10^{-4} \sqrt{\omega} \text{ m}^{-1}.$$
 (6)

The decay due to the big cylinders is enhanced by 11% in the SC as compared to the decay $\gamma_{\rm ph2}$ in the phononic crystal. Note that the ratio γ_2/γ_1 is close to the ratio of the cumulative areas of two types of the cylindrical surfaces in infinite supercrystal, $(R_2/R_1)(a_1/a_2)^2 \approx 0.057$. The latter can be written as $\frac{L_2}{A_{c_2}}/\frac{L_1}{A_{c_1}}$, that may be erroneously considered as weak

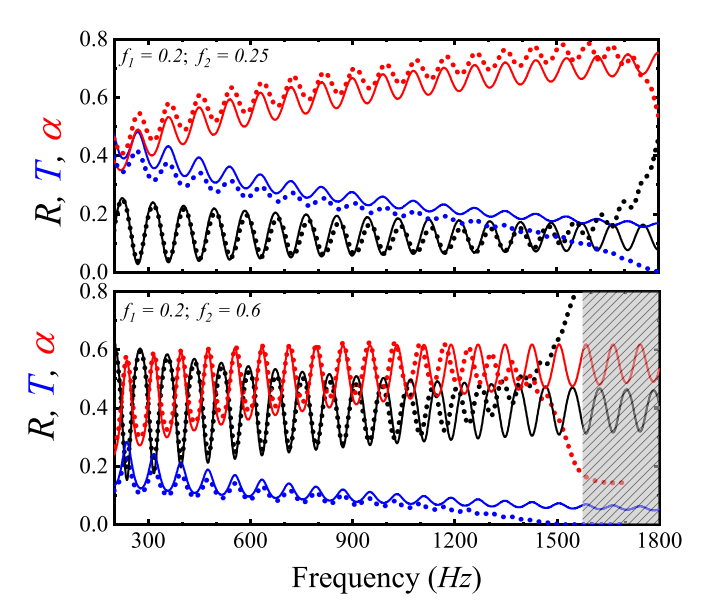


FIG. 2. Reflectance, transmittance, and absorbance spectra for two SC slabs of the same thickness $d=1.56\,\mathrm{m}$. Solid lines show analytically calculated spectra for the slab of homogeneous metafluid with the effective parameters of the corresponding SCs. Dotted lines show numerically calculated spectra for the finite-length SCs. For the SC with higher filling fraction of big cylinders (lower panel) their contribution to the decay coefficient $\gamma_{\rm sc}=0.0058\sqrt{\omega}$ is about 45% of the attenuation due to the background of the lattice of small cylinders. The shaded area marks the bandgap.

sensitivity of M/N to the geometry of the unit cell. However, this spurious independence is due to relatively low and close filling fractions of the lattices, $f_1 = 0.2$ and $f_2 = 0.25$.

According to Eq. (4) the total decay of sound in the SC is evaluated as

$$\gamma_{\rm sc} = \gamma_1 + \gamma_2 = 0.0048 \sqrt{\omega} \text{ m}^{-1}.$$
 (7)

Due to interlattice interaction the sound wave in the SC decays by 20% faster than in the phononic crystal of small cylinders.

The homogenized SC can be considered as a viscous metafluid with density $\rho_{\rm sc}=322.5~{\rm kg/m^3}$, elastic modulus $\lambda_{\rm sc}\approx\lambda_0/(1-f_1)(1-f_2)=0.254~{\rm MPa}$, and speed of sound $c_{\rm sc}=\sqrt{\lambda_{\rm sc}/\rho_{\rm sc}}=281~{\rm m/s}$. Its effective viscosity $\eta_{\rm sc}$ is introduced by equating $\gamma_{\rm sc}$ to the bulk decay coefficient $2\omega^2\eta_{\rm sc}/3\rho_{\rm sc}c_{\rm eff}^3$ of a homogeneous metafluid,

$$\eta_{\rm sc} = \frac{3\rho_{\rm sc}c_{\rm sc}^3}{2\omega^2}\gamma_{\rm sc} = \frac{0.51 \times 10^5}{\omega^{3/2}} \left(\frac{\rm kg}{\rm s\,m}\right).$$
(8)

Note that the effective viscosity exhibits anomalous dependence decaying with frequency. At frequency of 1 kHz, the SC behaves as a metafluid, which is approximately 5000 times more viscous than air.

The accuracy of the proposed theory is confirmed by numerically calculated spectra of sound transmission (T), reflection (R) and absorption (α) for a finite-length SC. The slab thickness $d=24\times\sqrt{3}a_2/2=1.56\,\mathrm{m}$, where 24 is the number of parallel layers of cylinders with the interlayer distance $\sqrt{3}a_2/2$ arranged in a hexagonal lattice, see Fig. 1. Numerically calculated spectra for two SC with the same lattice structure but different filling fractions are shown in Fig. 2 by

dotted lines. These spectra coincide well with the analytically calculated spectra (solid lines) for the homogeneous slab of the same thickness *d* with mechanical and dissipative effective parameters of the corresponding SC.

The numerical spectra are calculated in the thermoviscous boundary layer impedance approximation (BLI). The adiabatic condition was applied to exclude the thermic losses within the boundary layers around the scatterers [29]. This approximation is practically indistinguishable from the time-consuming full COMSOL calculations, since only very small part $\gamma_0/\gamma_{\rm sc} \sim 10^{-5}$ of acoustic energy is absorbed in the bulk of air matrix [27]. The analytical spectra of the homogeneous slabs are close to the numerical spectra even above the homogenization limit at 900 Hz [25]. Essential differences appear for the frequencies close to the band gap (>1.2 kHz). Oscillations on the graphs are due to the Fabry-Perot resonance at frequencies 90 and 79 Hz ($c_{\rm sc}/2d$) for the slabs representing two different SCs with effective speeds of sound of 281 and 247 m/s.

The viscous losses were measured using a 3D printed sample of ABS plastic with density 1.05 g/cm³. The parameters of the SC were selected to be exactly the same as reported in Ref. [15]: $a_1 = 2.5 \text{ mm}$, $a_2 = 33.7 \text{ mm}$, $R_1 =$ 1 mm, and $R_2 = 9.7$ mm. The SC thickness slab was d =30 mm. This slab contains 13 periods a_1 that is sufficient to measure the dispersive and dissipative parameters of the corresponding phononic crystal. However, only one layer of the big cylinders fits the slab, therefore some disagreement with the results obtained for infinite supercrystal is expected. The thickness of the slab is limited by the geometrical parameters of the standard circular cross-section acoustic impedance tube (ACUPRO) with driver JBL 2426H. A reference sample of thickness $d_r = 28.7 \,\mathrm{mm}$ with small cylinders only was 3D printed to demonstrate applicability of the results of the homogenization theory. The transfer-matrix method [30] was applied to extract the acoustic impedance $Z = \rho c$ and the complex wave number $k + i\gamma$ from the experimental data.

Since at frequencies below 1.5 kHz the typical decay length of sound $1/\gamma_{\rm sc} \sim 0.5 \, \rm m$ is much larger than the 3D printed sample size d, the attenuation of sound signal is relatively low, while it is 4-5 orders of magnitude stronger than in air. The values of the decay coefficient were extracted from the measurements of acoustic impedances of the SC sample and of the reference phononic crystal with period a_1 . The results are shown in Fig. 3. The effective parameters of the fabricated SC calculated for infinite sample are: $\rho_{\rm sc} = 8.39$ kg/m³, $c_{sc} = 241$ m/s, and $\gamma_{sc} = 0.021 \sqrt{\omega}$ m⁻¹. For the sample of phononic crystal of small cylinders (the background medium), they are $\rho_{bg} = 4.54 \text{ kg/m}^3$, $c_{bg} = 274 \text{ m/s}$, and $\gamma_{bg} = 0.018 \sqrt{\omega} \text{ m}^{-1}$. It is seen from Fig. 3 that the correspondence between the theory and experiment is better for the slab of phononic crystal than for the supercrystal sample because of lack of periodicity in the latter case. For both experimental samples, the frequency dependence of the normalized decay coefficient follows the analytical result $\gamma_{\rm sc}/\gamma_0 \propto \omega^{-3/2}$. It is natural that the numerical results accounting for thermoviscous losses (dashed curve) are closer to the experimental data, especially for the phononic crystal sample. By the same reason the analytical curves are closer to the numerical data

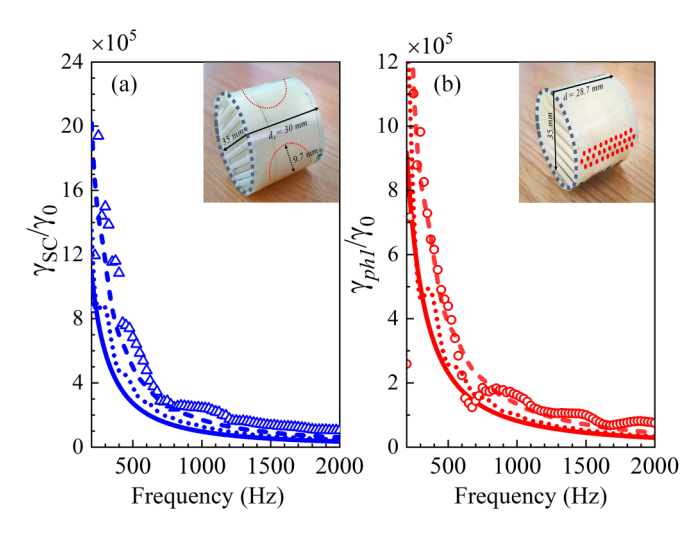


FIG. 3. Comparison of the experimental, numerical and analytical spectra for the normalized decay coefficient in a supercrystal (a) and in a phononic crystal of small cylinders with period $a_1 = 2.5 \, \text{mm}$ (b). The experimental data (symbols) are obtained by measuring the acoustic impedance of the slabs of thicknesses 30 mm (supercrystal) and of 28.7 mm (phononic crystal). The analytical results (continuous lines) are calculated for the corresponding infinite structures. The numerical spectra are calculated in the BLI approximation separately for pure viscous (dotted curve) and thermoviscous (dashed curve) losses of a supercrystal (a) (10 layers of big cylinders) and of a phononic crystal (b) (300 layers of small cylinders). The insets show photos of the supercrystal and phononic crystal samples.

accounting only viscous losses. It is seen from Fig. 3 that the contribution of thermal losses may reach 10% at low frequencies. Note that the homogenization theory proposed here justifies the phenomenologically predicted enhanced inertia in a lossy supercrystal [15].

In conclusion, we propose a theory for calculation of the effective parameters of a 2D lossy phononic SC, i.e., a structure of elastic rods with doubly periodicity in a viscous fluid matrix. Frequency-dependent effective viscosity is introduced for phononic crystal with arbitrary 2D Bravais lattice and arbitrary cross-section of cylindrical inclusions. Theoretical predictions are confirmed by numerical simulations and partially by experimental results. Some disagreement observed between theory and experiment is attributed to insufficient length of the SC sample used in the experiment. At the same time, the experimental results obtained for the phononic crystal with many periods, which serves as the background medium for the supercrystal, are in a better agreement with the theory. In addition, Fig. 3 indicates that the experimental values of the decay coefficient are higher than the theory predicts. We attribute this difference to the fact that thermal losses in water are omitted in the proposed theory.

The proposed theory is applicable for design of metafluids with prescribed elastic parameters and enhanced dissipative losses. In addition, it is valid for lattices with low rotational symmetry, which in the low-frequency limit behave as anisotropic metafluids. In these structures viscosity becomes a fourth-rank tensor where the odd viscosity effects theoretically predicted for hypothetical anisotropic fluids may be observed [31].

This work is supported by the NSF Grant No. 1741677 and by the AFOSR Grant No. FA9550-23-1-0630. M.I. is thankful

to Instituto de Física Universidad Autónoma de Puebla and to J. Arriaga for computer facilities.

- L. D. Landau and E. M. Lifshitz, *Fluid Mechanics* (Elsevier, Oxford, 1984).
- [2] M. I. Hussein and M. J. Frazier, Metadamping: An emergent phenomenon in dissipative metamaterials, J. Sound Vib. 332, 4767 (2013).
- [3] C. Lagarrigue, J. P. Groby, V. Tournat, O. Dazel, and O. Umnova, Absorption of sound by porous layers with embedded periodic arrays of resonant inclusions, J. Acoust. Soc. Am. 134, 4670 (2013).
- [4] D. M. Garza-Agudelo, V. Cutanda Henriquez, C.-H. Jeong, and P. R. Andersen, Characterization and optimization of the angle dependent acoustic absorption of 2D infinite periodic surfaces of Helmholtz resonators, J. Theor. Comp. Acout. 31, 2250010 (2023).
- [5] X. H. Zhang and Z. G. Qu, Viscous and thermal dissipation during the sound propagation in the continuously graded phononic crystals, Appl. Acoustics 189, 108606 (2022).
- [6] S. Wang, B. Hu, and Y. Du, Sound absorption of periodically cavities with gradient changes of radii and distances between cavities in a soft elastic medium, Appl. Acoustics 170, 107501 (2020).
- [7] X. H. Zhang, Z. Qu, and H. Wang, Engineering acoustic metamaterials for sound absorption: From uniform to gradient structures, iScience 23, 101110 (2020).
- [8] V. Romero-García, N. Jiménez, J.-P. Groby, A. Merkel, V. Tournat, G. Theocharis, O. Richoux, and V. Pagneux, Perfect absorption in mirror-symmetric acoustic metascreens, Phys. Rev. Appl. 14, 054055 (2020).
- [9] S. Huang, Z. Zhou, D. Li, T. Liu, X. Wang, J. Zhu, and Y. Li, Compact broadband acoustic sink with coherently coupled weak resonances, Sci. Bull. 65, 373 (2020).
- [10] J.-P. Groby, A. Wirgin, L. De Ryck, W. Lauriks, R. P. Gilbert, and Y. S. Xu, Acoustic response of a rigid-frame porous medium plate with a periodic set of inclusions, J. Acoust. Soc. Am. 126, 685 (2009); J.-P. Groby, O. Dazel, A. Duclos, L. Boeckx, and L. Kelders, Enhancing the absorption coefficient of a backed rigid frame porous layer by embedding circular periodic inclusions, *ibid.* 130, 3771 (2011).
- [11] C. R. Liu, J. H. Wu, Z. Yang, and F. Ma, Ultra-broadband acoustic absorption of a thin microperforated panel metamaterial with multi-order resonance, Compos. Struct. **246**, 112366 (2020).
- [12] X. Li, B. Liu, and Q. Wu, Enhanced low-frequency sound absorption of a porous layer mosaicked with perforated resonator, Polymers 14, 223 (2022).
- [13] A. Climente, D. Torrent, and J. Sánchez-Dehesa, Omnidirectional broadband acoustic absorber based on metamaterials, Appl. Phys. Lett. 100, 144103 (2012); V. C. Henríquez, and J. Sánchez-Dehesa, Viscothermal effects in a two-dimensional acoustic black hole: A boundary element approach, Phys. Rev. Appl. 15, 064057 (2021).
- [14] Y. A. Godin, Effective complex permittivity tensor of a periodic array of cylinders, J. Math. Phys. **54**, 053505 (2013).

- [15] M. D. Guild, V. M. Garcia-Chocano, W. Kan, and J. Sánchez-Dehesa, Enhanced inertia from lossy effective fluids using multi-scale sonic crystals, AIP Adv. 4, 124302 (2014).
- [16] M. D. Guild, V. M. Garcia-Chocano, W. Kan, and J. Sánchez-Dehesa, Acoustic metamaterial absorbers based on multilayered sonic crystals, J. Appl. Phys. 117, 114902 (2015).
- [17] M. Ibarias, Y. Zubov, J. Arriaga, and A. A. Krokhin, Phononic crystal as a homogeneous viscous metamaterial, Phys. Rev. Res. 2, 022053(R) (2020).
- [18] M. Ibarias, J. Doporto, A. A. Krokhin, and J. Arriaga, Tuning the decay of sound in a viscous metamaterial, Phil. Trans. R. Soc. A. 380, 20220007 (2022).
- [19] D. Shymkiv and A. Krokhin, Effects of viscous dissipation in propagation of sound in periodic layered structures, J. Acoust. Soc. Am. 155, 990 (2024).
- [20] C.-Y. Lee, M. J. Leamy, and J. H. Nadler, Frequency band structure and absorption predictions for multi-periodic acoustic composites, J. Sound Vib. 329, 1809 (2010).
- [21] E. E. Narimanov, Photonic hypercrystals, Phys. Rev. X 4, 041014 (2014).
- [22] Q. Yao, L. Liu, S. Malola *et al.*, Supercrystal engineering of atomically precise gold nanoparticles promoted by surface dynamics, Nat. Chem. 15, 230 (2023).
- [23] K. Aryana and M. B. Zanjani, Diamond family of colloidal supercrystals as phononic metamaterials, J. Appl. Phys. 123, 185103 (2018).
- [24] A. A. Krokhin, J. Arriaga, and L. N. Gumen, Speed of sound in periodic elastic composites, Phys. Rev. Lett. 91, 264302 (2003).
- [25] D. Torrent, A. Håkansson, F. Cervera, and J. Sánchez-Dehesa, Homogenization of 2D clusters of rigid rods in air, Phys. Rev. Lett. **96**, 204302 (2006).
- [26] Y. Wu, Y. Lai, and Z.-Q. Zhang, Effective medium theory for elastic metamaterials in two dimensions, Phys. Rev. B **76**, 205313 (2007).
- [27] See Supplementary Material at http://link.aps.org/supplemental/ 10.1103/PhysRevResearch.6.L042005 for the details of calculations of the effective parameters (speed of sound and decay coefficient) for 2D phononic crystal.
- [28] D. Torrent and J. Sánchez-Dehesa, Anisotropic mass density by 2D acoustic metmaterials, New J. Phys. 10, 023004 (2008); L. N. Gumen, J. Arriaga, and A. A. Krokhin, Metafluid with anisotropic dynamic mass, Low Temp. Phys. 37, 975 (2011).
- [29] M. J. Cops, J. G. McDaniel, E. A. Maglius, D. J. Bamford, and M. Berggren, Estimates of acoustic absorption in porous materials based on viscous boundary layers modeles as boundary conditions, J. Acoust. Soc. Am. 148, 1624 (2020).
- [30] B. H. Song and J. S. Bolton, A transfer-matrix approach for estimating the characteristic impedance and wave numbers of limp and rigid porous materials, J. Acoust. Soc. Am. 107, 1131 (2000).
- [31] J. E. Avron, Odd viscosity, J. Stat. Phys. 92, 543 (1998); X. M. de Wit, M. Fruchart, T. Khain, F. Toschi, and V. Vitelli, Pattern formation by turbulent cascades, Nature (London) 627, 515 (2024).